National Physical Laboratory

NPL REPORT MAT 116

RAPID MAPPING OF MECHANICAL PROPERTIES OF AM SAMPLES WITH INDENTATION

H. ZHANG, C. GREEN, P. WOOLLIAMS, J. NUNN, K. P. MINGARD, A. T. FRY

DECEMBER 2022

Department for Business, Energy & Industrial Strategy

FUNDED BY BEIS

Rapid mapping of mechanical properties of AM samples with Indentation

H. Zhang, C. Green, P. Woolliams, J. Nunn, K. P. Mingard, A. T. Fry
Advanced Engineering Materials

ISSN 1754-2979

https://doi.org/10.47120/npl.MAT116

National Physical Laboratory
Hampton Road, Teddington, Middlesex, TW11 0LW

This work was funded by the UK Government's Department for Business, Energy and Industrial Strategy (BEIS) through the UK's National Measurement System programmes.

Approved on behalf of NPLML by
Stefanos Giannis, Science Area Leader Advanced Engineered Materials.

CONTENTS

1 INTRODUCTION

For efficient energy use and maximising performance using materials which exhibit a high strength to weight ratio is of considerable importance for automotive and aerospace products. For metallic materials one approach to do this is to use high strength light alloys such at titanium, magnesium and aluminium for structural use, or for less structurally demanding application one can manufacture pores into the material, for example by the production of metallic foams. Traditionally, it is difficult and expensive to fabricate structures with a controllable number of pores, to enable the optimisation of weight. In addition, the rapid development of complex, near net shaped parts in industrial applications is becoming an increasingly important consideration with the drive to more sustainable and efficient manufacturing routes. The laser powder bed manufacturing (LPBF) process used in additive manufacturing (AM) offers rapid solidification with fast cooling rates and tuneable processing conditions to enable design optimisation of microstructures and morphologies which have the potential to be exploited to provide tailored and specific material properties. With such degrees of freedom in the manufacturing process it is critical for users of this manufacturing technique to be confident that they are using appropriate processing parameters. This report describes the work conducted to design and evaluate a sample for the rapid measurement and mapping of the processing windows for LPBF materials. To illustrate and evaluate the sample design and methodology two aluminium alloys have been selected and used.

The highly localised heating and consolidation effects in the LPBF process can result in a microstructure that is anisotropic and can have associated defects such as pores, trapped powder, 'kissing bonds' etc. The approach presented here uses simple specimens, optical and electron microscopy and indentation techniques to map the morphological structure and mechanical properties to correlate these with the processing parameters used in the manufacture of the sample to allow industrial users to narrow down and optimise the processing parameters for their own specific material and machine combinations.

2 SAMPLE DESIGN

To understand the influence that different process conditions would have on the material properties (density, appearance, morphology, elastic modulus), a simple sample and analysis approach has been developed. A simple cuboid sample consisting of a 7x7 grid array was designed which could be easily manufactured by using different processing parameters for each square section of the grid array. This removes the need and cost of manufacturing traditional tensile samples, allowing for a wider range of process conditions to be rapidly assessed.

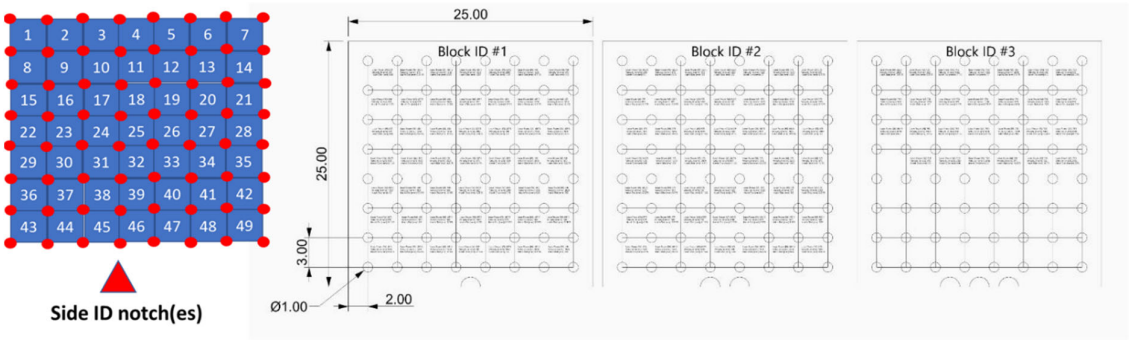

Figure 1 Schematic of the process parameter sweep sample design

The design of the sample is shown in Figure 1. This shows the grid array where each sub-cube was 3x3x3mm in size with thin gaps between to allow easy identification of the specific cubes. Indents were used on one edge of the sample to provide identification and sample orientation, as shown in the three samples to the right hand side of Figure 1.

A design of experiments approach was taken to scan over a range of laser power, beam travel speed and hatch spacing, the layer height was taken as the standard that the LPBF machine used. With 5 variations of each parameter, a total of 125 different combinations were created, these were randomly distributed across three different cube array samples with some repeats to make up the total 147 cubes.

The energy density for each process condition was calculated (Equation 1) as well as the relative deposition speed (Equation 2)

$$Relative\ energy\ density = \frac{Laser\ Power}{Hatch\ spacing\ x\ laser\ velocity}$$

Equation 1

$$Relative\ deposition\ speed = \frac{Laser\ velocity}{Hatch\ spacing}$$

Equation 2

Figure 2 shows the variation of the energy density and deposition speed for all the process conditions tested, in this case it was for the Scalmalloy [1] material, described in the following sections.

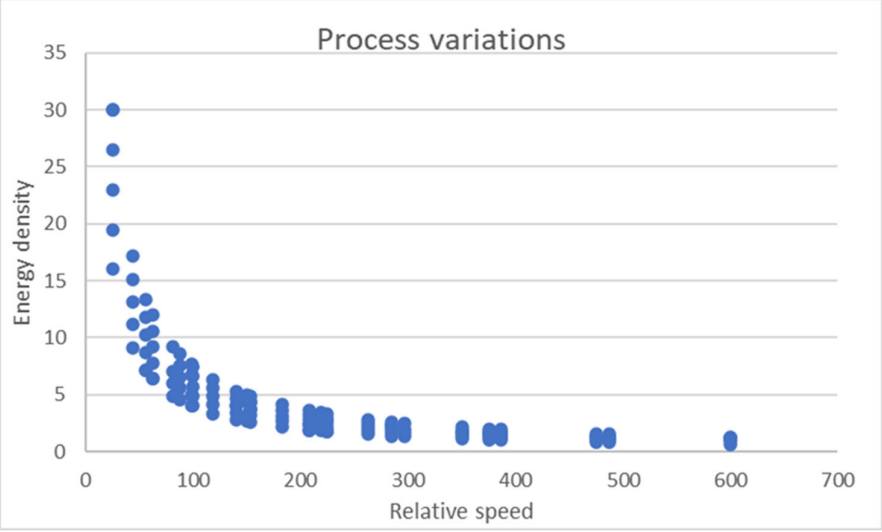

Figure 2 Variation in energy density with the relative speed

3 ANALYSIS TECHNIQUE

Once manufactured, images of the samples were taken and then the samples were embedded in hot-mount resin and the top millimetre of the sample was ground and polished back to expose

a cross-section that was representative of the bulk material. An example of three samples prepared in this manner is shown in Figure 3. Figure 4 shows one of the samples in the mount after the grinding and polishing procedure.

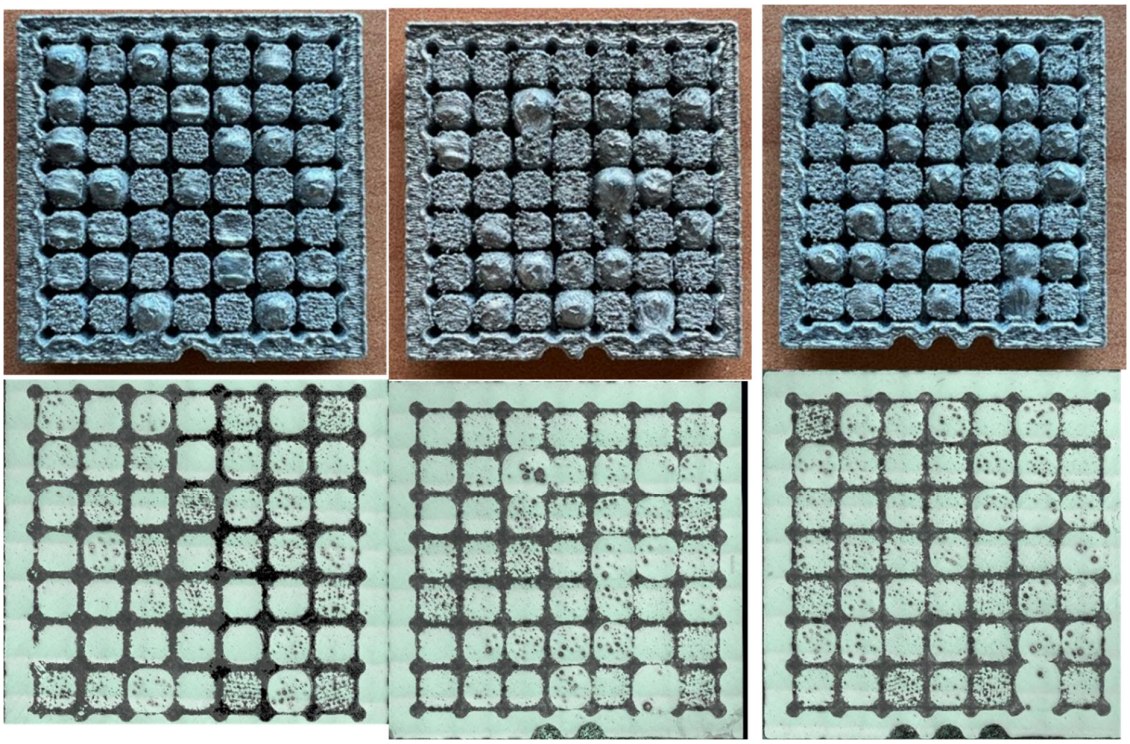

Figure 3 Images for three samples in the as manufactured condition (top) and an image after polishing (bottom)

It was clear that the samples with extreme energy densities showed either evidence of boiling (too high energy density, the cube merged with the surrounding ones and contained large spherical pores) as seen in images of the as manufactured sample in the top row of Figure 3 or lack of fusion (with significant amounts of largescale porosity from where the laser was unable to melt the powder particles together) as visible in the images of polished samples in the bottom row of Figure 3.

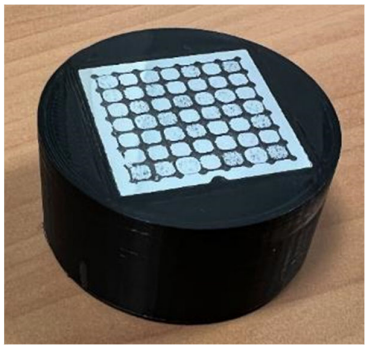

Figure 4 Mounted and polished sample

The porosity level of each of the process conditions was measured by thresholding an optical microscope image of the polished sample (Figure 4) and selecting central regions of each cube. This allowed the range of conditions that provided the lowest porosity to be identified and the

conditions where excess energy density was deposited to be eliminated from further consideration.

For the purposes of this work a range of process conditions were selected that enabled material deposition at increasing rates with diminishing mechanical performance as required. To aid the choice of process combinations, the laser power was fixed at a value that resulted in the lowest porosity in the porosity vs relative speed plot (all combinations that involved deposition rates slower than the lowest porosity combination were also eliminated). Figure 5 presents a summary of the measured porosity (from the optical micrographs) as a function of the energy density. Two regions have been identified on this plot which show where excessive 'boiling' of the material occurred and where there were high levels of lack of fusion.

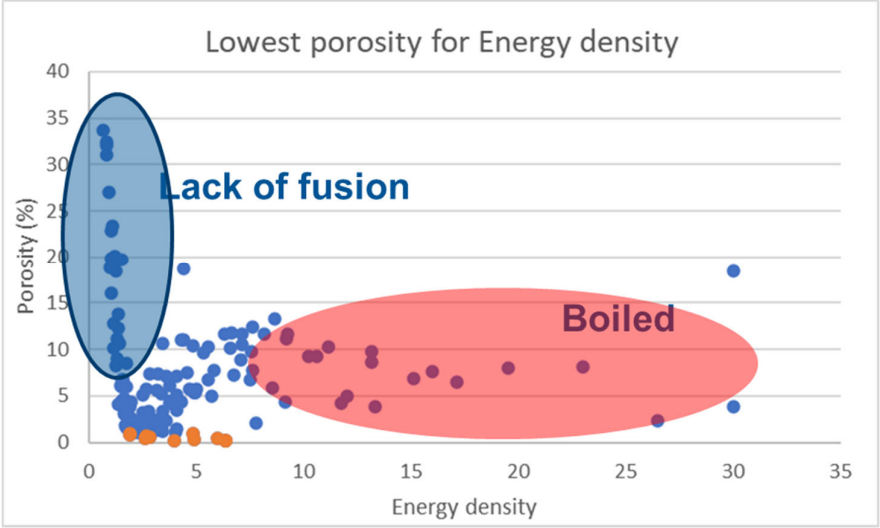

Figure 5 Summary of the measured porosity as a function of the energy density

A subset of the data has been additionally plotted in Figure 6 showing how the porosity varies as a function of the relative print speed for a fixed laser power of 487.5W.

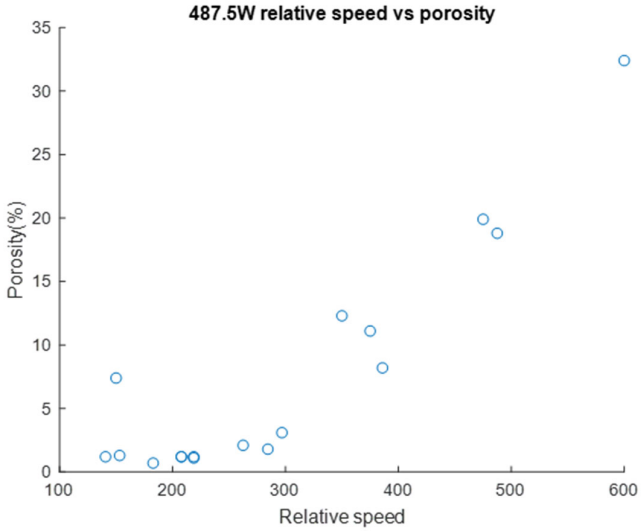

Figure 6 Selected data of porosity as a function of relative speed

These cubes were then subjected to mapping using a quick indentation scanning method with the NPL Scanning Indentation Microhardness Measurement system (SIMM), where elastic and plastic properties are reflected from the indentation load-displacement curves.

4 INDENTATION METHODOLOGY

Indentation techniques using the NPL SIMM and to a lesser degree instrumented indentation testing (ITT) have been applied to investigate the correlation between the processing condition and the mechanical and physical properties. As semi-destructive tests, SIMM and IIT require nearly no sample preparation and can be performed on the final product. They can be used to achieve a thorough multiscale measurement from sub-micron to bulk mechanical response reflected in the load-displacement curve, and via quantified data in terms of hardness and Young's modulus.

4.1 SCANNING INDENTATION MICROHARDNESS MEASUREMENT SYSTEM (SIMM)

Using the sample described previously, a methodology has been developed to rapidly extract the mechanical data as a function of processing parameters to help industry optimise the manufacturing window. Large micro indentation arrays have been performed to investigate the mechanical variation within the sample and as a function of processing parameters.

The NPL SIMM offers a relatively high-speed facility to map large areas quickly. Maps can be formed from an X by Y array of indentations. Typically, an area of 7.5mm x 20mm can be characterised with 17,000 indents. These can be placed on a square array with each indent separated by about 100 μm, and typically would use a load of 0.2 N. Under these conditions for a steel material the indent diameters are typically 20 μm. Maps can be generated automatically by leaving the machine to run continuously over a period of ~37 hours for this number of indents.

In the SIMM force and displacement are monitored continuously during a complete indentation cycle, which can typically be completed in 15s.

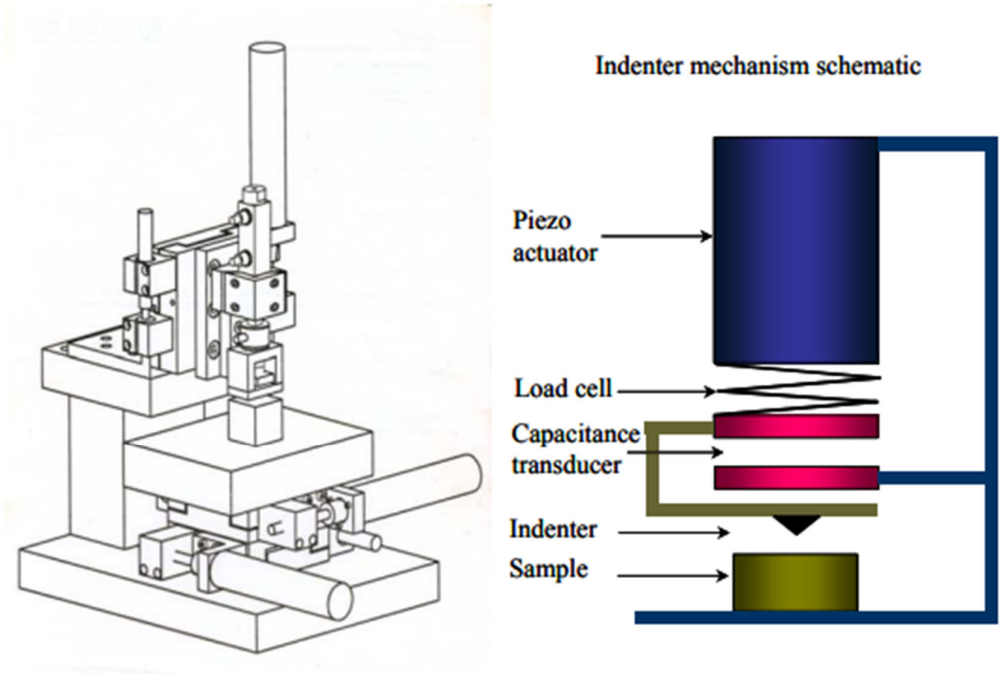

Figure 7 Schematic diagram of SIMM

Three linear slides provide the X, Y and Z movement, (Figure 7). Each slide is driven by a 1 mm pitch screw thread, powered by a servo-controlled DC motor. A microprocessor controller determines the position of each slide with one micrometre resolution. Control feedback is via a 500-line rotary encoder attached to the shaft of each motor. The load is measured with a conventional strain gauged load cell, and the Vickers indenter was taken from a conventional microhardness system. The loading mechanism uses a piezoelectric actuator. A piezoelectric system has the potential to be quick, with a high resolution. However, the main drawback is a limited range of movement of around 60 μm. The complete assembly is mounted on a motorised Z stage. The motor is driven to within a few micrometres of the surface, and the piezoelectric mechanism is used to perform the indentation. From this position the Z motor is only used to accommodate any roughness or misalignment of the sample surface. To operate the system the piezoelectric actuator is expanded by the application of a high voltage, and this causes the indenter to move towards the sample. The motion of the indenter is measured by the capacitance transducer and is a measurement relative to a static capacitance plate which is in turn mechanically connected to the sample surface. When the indenter touches the sample surface a load is registered on the load cell. Loading is continued until the desired load is reached. The design of the loading mechanism is such that although the strain gauge load cell is effectively a soft spring, the compression of the load cell does not register on the displacement measurement system as the load cell is above the capacitance transducers. This means that there is no need to correct for the load cell stiffness in the final load against displacement curves.

The principles of depth sensing hardness at the macroscopic level (i.e. application loads of typically 5-20 N) have been extensively demonstrated by Thurn et al [2] on a range of ceramic materials. For the depth sensing hardness HV (SIMM) is defined by P/A, where A is the projected area of contact, and this is calculated from

$$HV\ (SIMM) = P/(24.5^* (h_c + h_o)^2)$$

Equation 3

where h_c is the indentation contact depth under load (Figure 8), and h_o is a depth offset which caused by the imperfection of the indenter tip (i.e., wear of the indenter tip), which needs to be determined by measurement on reference materials. The hardness at each point is determined by using the following method on the load/displacement curves.

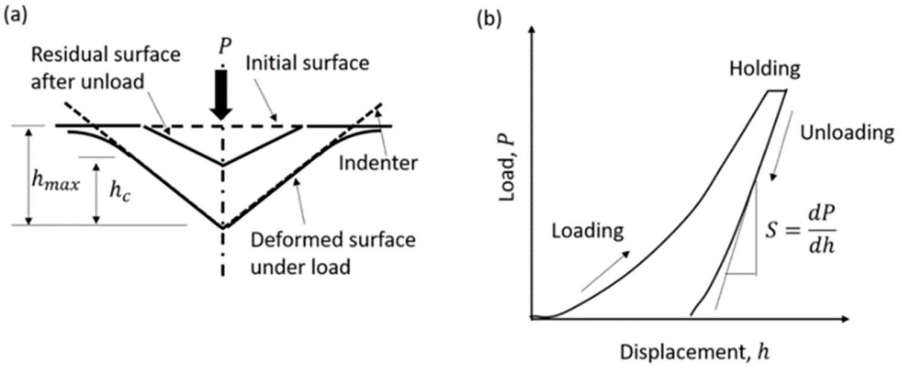

Figure 8 Schematic of indentation (a) and corresponding load-displacement curve (b)

Firstly, the surface is found by fitting a polynomial to the initial 5% of the loading curve. This is followed by finding h_{max}, the depth at maximum load. A linear fit to the top 20% of the unloading curve is then extrapolated down to zero load, to give the unloading displacement, h_r. The indentation contact depth under load, h_c, is then determined using

$$h_c = h_{max} - 0.75*(h_{max}-h_r)$$

Equation 4

The major difference between the method adopted for the NPL machine and the ISO guidelines is that the data from the NPL machine was not corrected for the machine compliance, since a satisfactory method for this correction has yet to be determined, further details on the SIMM can be found the NPL Measurement Note DEPC-MN 30 [3].

Full recalibration of the SIMM can be performed and involves:

- A full recalibration of the loadcell (up to 2.5N), using a special loading jig and an air bearing and calibrated masses, with residuals after cubic fitting of within 0.015N.
- Calibration of the capacitance sensor, against another calibrated displacement sensor, with residuals <20 nm.
- Measurement of tip geometry using a Scanning Electron microscopy to confirm that the ridge at the tip of the Vickers indenter was about 300 nm long, for the indent depth of a few micrometres, a ridge length of up to 500 nm is considered acceptable (for instance micro hardness testing). The calibration against reference materials indicates an offset of about 90 nm for the current indenter.

A complete redetermination of the system compliance was deemed unnecessary, the existing corrections were kept.

As built the SIMM was designed to apply the ramped test load and then immediately unload the sample to allow it to make as many indents as rapidly as possible, as quite often very large

numbers are needed for scanning large samples and relative results were deemed more important.

A check was made between the results from the SIMM and a macro-indenter which initially identified some differences. These differences were due to the SIMM not holding the load on the indenter as undertaken in standard hardness testing, where the samples can "creep" slightly. The SIMM control software was updated to enable the user to specify a variable length "hold" duration, with repeat comparisons to demonstrate the agreement in hardness measurements to macro hardness instruments using calibrated refence materials, Figure 9

Figure 9 Comparison of SIMM and macro hardness measurements, with improvement due to additional of "hold" period

A new guidance document was written to ensure future recalibrations are carried out in the same way.

During testing it was noted that the SIMM sometimes "crashed" and stopped measuring on porous samples and sometimes left behind scratches on the edges of metal samples when mounted in resin. The control logic for surface finding and tracking was updated and made more robust, so that it will not get stuck in pores and is more robust to height offsets between metal samples and the mounting resin. An example of a successful scan is shown in Figure 10.

When high levels of porosity are present, the indenter can still complete the measurements but if the measurement is obtained within a pore the measurements tend to be softer and the full load displacement trace is often truncated. This can be alleviated by using a larger indenter such that a wider area is averaged over and there is less opportunity for the indenter to hit a pore.

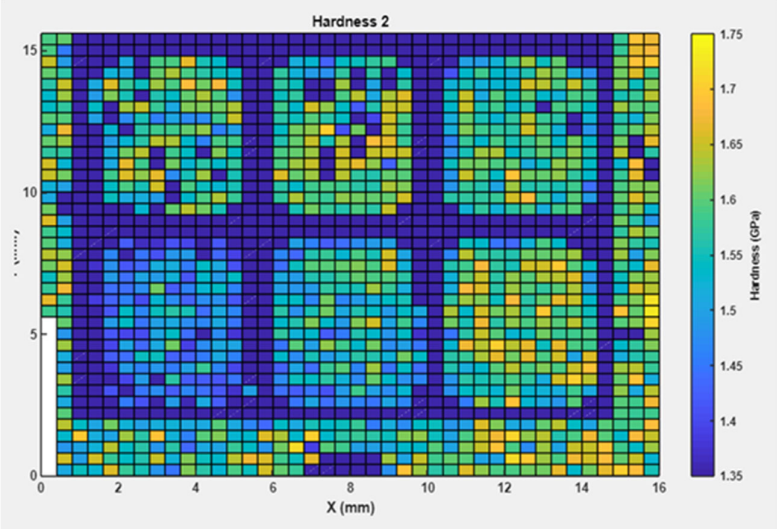

Figure 10 Example hardness map of an Aluminium process mapping sample

5 APPLICATION OF APPROACH – CASE STUDY

In this section, the experimental observations of the micro-defect-structure and mechanical behaviour of two additively manufactured aluminium alloys are presented. The use of the rapid processing parameter evaluation sample and analysis approach is demonstrated.

Three parameter sweep samples were manufactured using a range of processing conditions, as shown in Figure 5 and Figure 6, an example of the manufacture sample is shown in Figure 4. The SIMM was used to produce an array of micro indentation measurements as shown in Figure 11. It can be seen in Figure 11 that the hardness values shown in (a) map very well to the porosity structure in the sample (b). Figure 12 shows an example of one of the maps in greater detail. In this figure you can see the hardness map and associated macroscopic and microscopic view of the indent arrays. This shows how the hardness values vary as a function of both the porosity in the sample and also as a function of interaction of melt pool boundaries, where the hardness would be expected to vary depending on whether it is within the 'pool' or at the boundary between 'pools'.

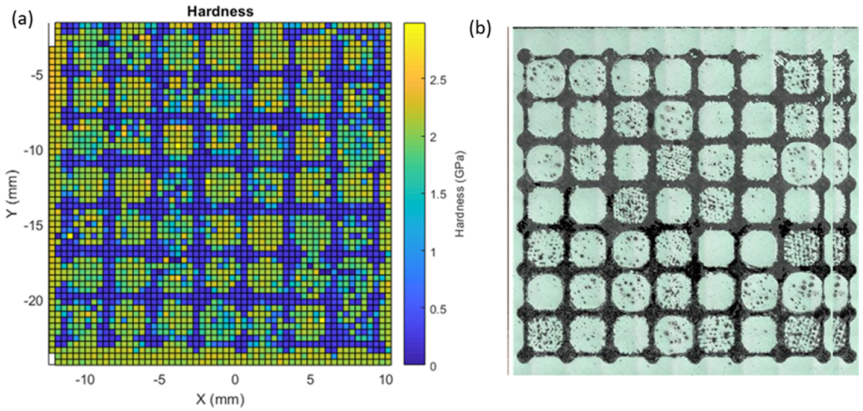

Figure 11 SIMM micro indentation map of samples under different deposition parameters showing (a) the hardness values and (b) optical image of the sample showing the porosity

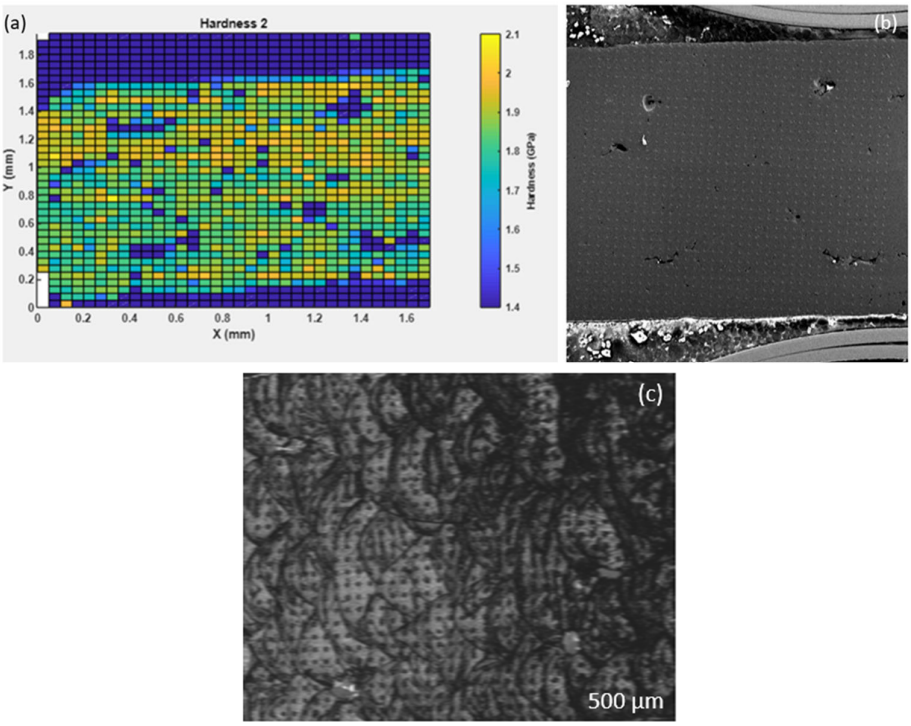

Figure 12 SIMM scanning (0.04 x 0.04 mm interval) of one scalmalloy sample (a) hardness values at different locations, (b) scanning electron microscope image of the indents corresponding to the SIMM mapping and (c) detailed information showing indents on individual melt pool and boundaries

With a large amount of data in the maps it is important to be able to generate meaningful statistics easily. To do this a MATLAB analysis method was developed shown in Figure 13 for a map generated for AlSi10Mg alloy. This shows the elastic modulus as a function of position on the sample, with each region being a different set of processing parameters. The figure shows histograms of the modulus and hardness values demonstrating the distribution across the sample allowing the user to home into the appropriate processing conditions for the desired properties.

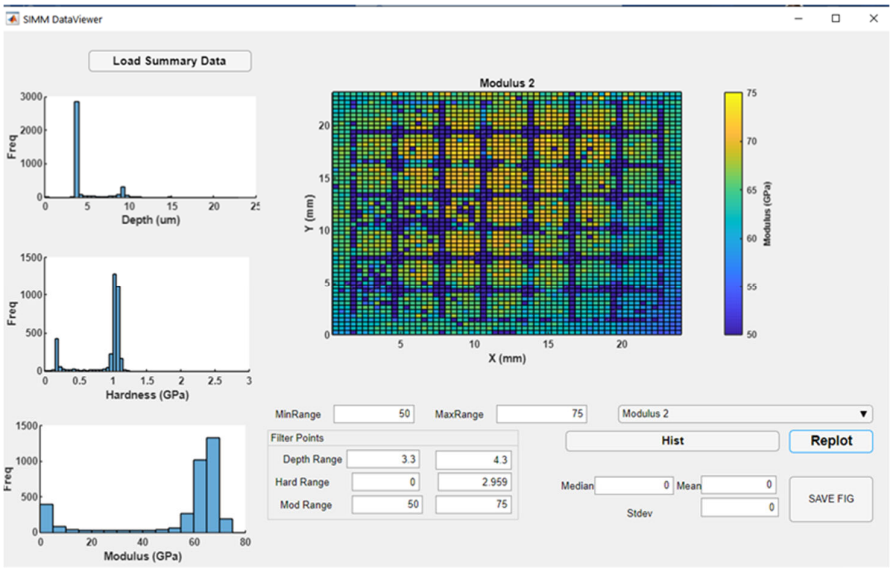

Figure 13 SIMM map showing the elastic modulus as a function of position on the sample. Also shown are the statistics for the modulus values for the indentation map on a AlSi10Mg sample

This approach was used for generating an appropriate range of processing parameters for a study on Scalmalloy. Samples as previously described were manufactured and used to isolate a set of seven processing conditions for further analysis using impact excitation, density measurement and tensile testing. This set of seven conditions was selected from the middle zone shown in Figure 5 where the material did not exhibit lack of fusion or boiling. These are shown, numbered, in Figure 14 which show the porosity as a function of manufacturing speed for a fixed laser power of 487.5W.

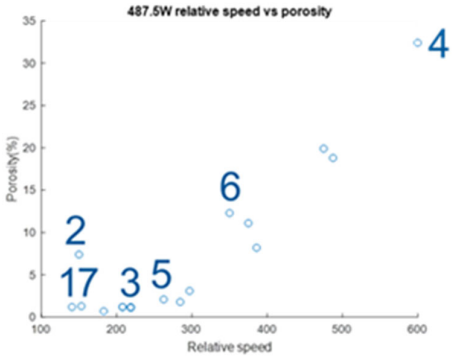

Figure 14 Porosity as a function of manufacturing speed for a fixed laser power of 487.5W for Scalmalloy

Impact excitation was used to measure the density of beam samples of the manufactured material for each of the seven processing conditions to determine the relative spread in the values. These values were compared to those from the standard alloy. The sample naming convention for all eight conditions is shown in Table 1. The results of the density measurements are presented in Figure 15 as a function of deviation from the standard alloy. It can be seen from this figure that the faster processing conditions resulted in a less dense build. This was also observable and illustrated in the processing sweep sample shown in Figure 11 and Figure 14. The effect of the degree of porosity or lower density can be seen in the relative elastic modulus values for the samples as shown in Figure 16. There is a ~60% reduction in the

stiffness of samples AJAR003 (processing ID 2), AJAR005 (processing ID 4) and AJAR007 (processing ID 6).

Miniature tensile tests pieces were manufactured using the 8 processing conditions and tested using a 50kN benchtop Instron Universal Test Machine. The results of these tests are presented in Figure 17, which shows how the strength and ductility changes as a function of processing parameters, porosity and density.

Table 1 Sample ID for the eight different processing conditions

Sample ID	Processing ID	Comment
AJAR001	0	Standard
AJAR002	1	Slowest
AJAR003	2	
AJAR004	3	
AJAR005	4	Fastest
AJAR006	5	
AJAR007	6	
AJAR008	7	

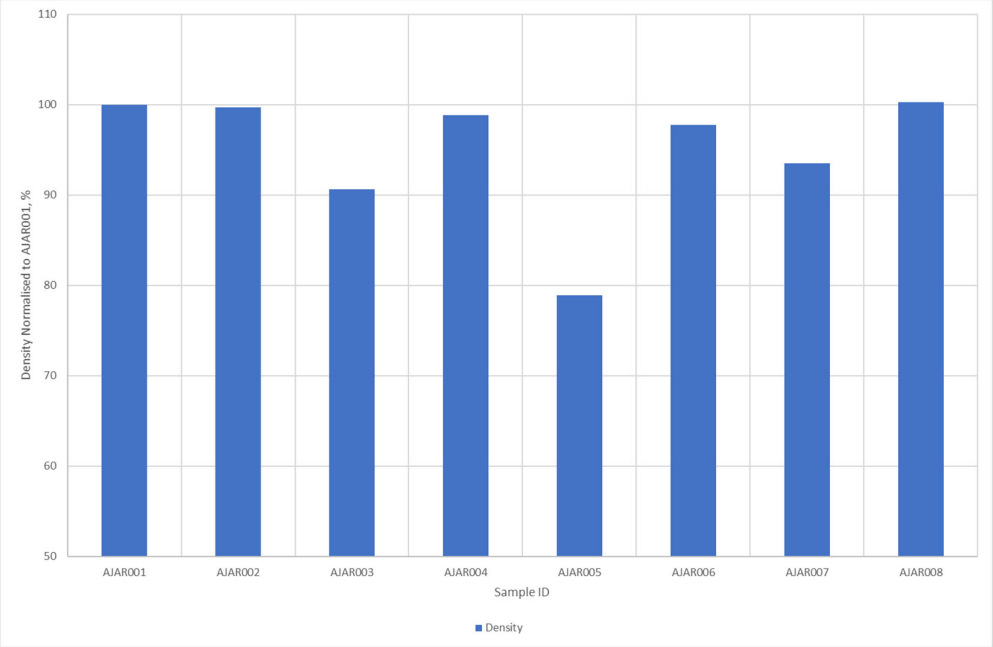

Figure 15 Relative density normalised against the standard processing parameters

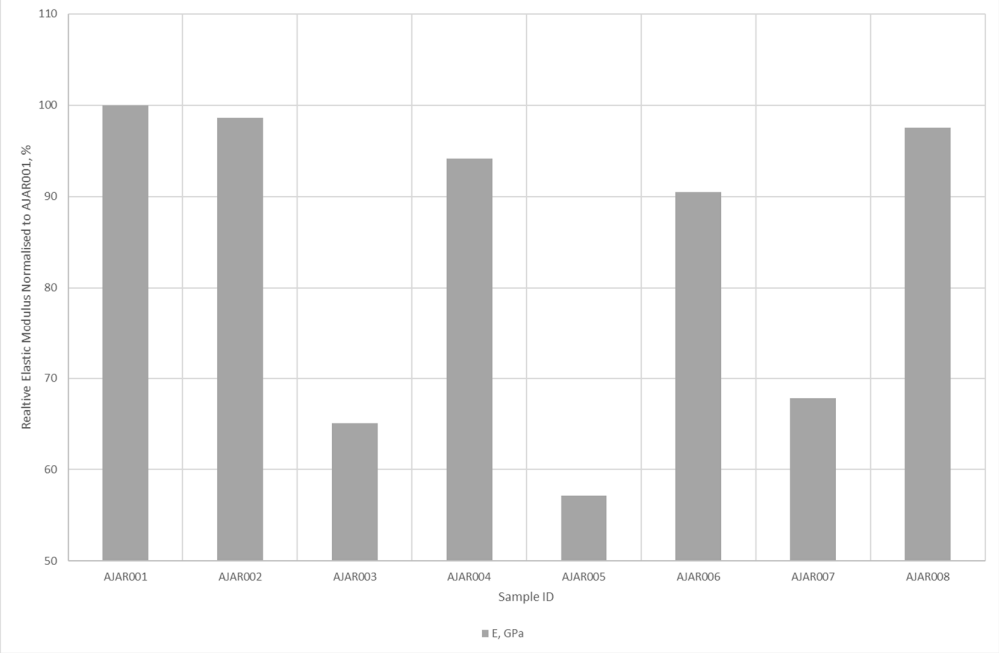

Figure 16 Relative elastic modulus normalised against the standard processing parameters

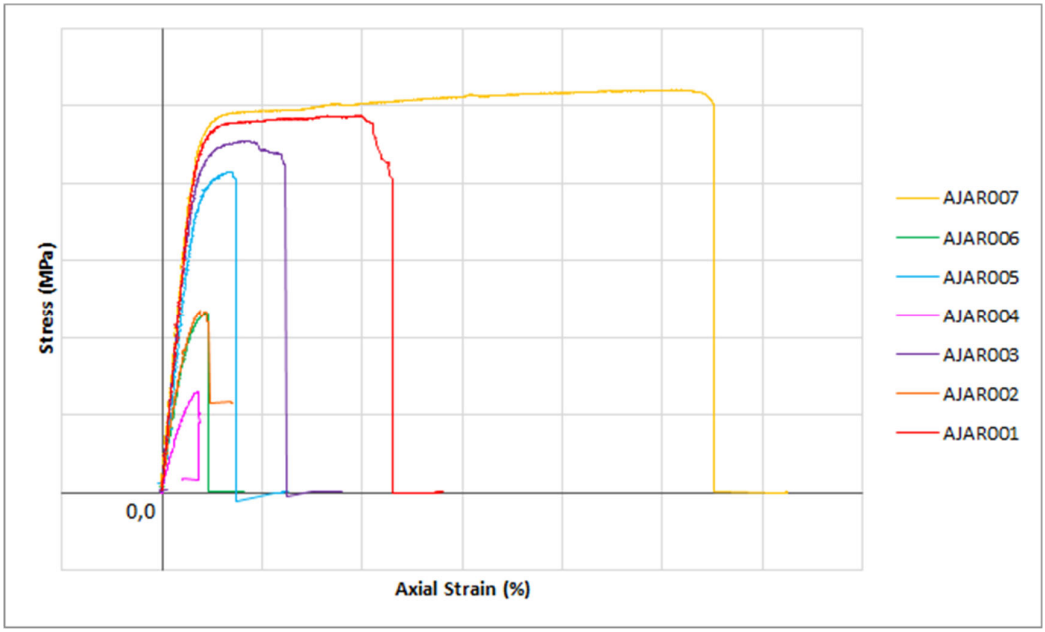

Figure 17 Stress vs strain plots for the different processing conditions (data values removed for commercial reasons)

6 CONCLUSIONS

The SIMM has been shown to be able to provide material modulus measurements that correlate well with other optical and mechanical techniques, though when a high level of porosity is present the ability of the SIMM to make the measurements degrades. This can be alleviated by using a larger indenter such that a wider area is averaged over and there is less opportunity for

the indenter to hit a pore. Despite this issue the SIMM performed well and has shown that using this approached coupled with simple optical evaluation can provide a rapid method to assess a wide range of processing parameters. It has the potential to offer a greater degree of discrimination between nominally identical macrostructures (in terms of % porosity and density).

For further evaluation of the material properties, it is possible to use impact excitation as a rapid evaluation measurement of density, axial modulus and shear modulus. This does require the manufacture of the beam sample but has the advantage of being able to measure the modulus of the sample as a function of temperature using only one specimen. It has also been shown that the application of miniature tensile tests can provide the final step of the process parameter evaluation.

7 FURTHER WORK

NPL will take delivery of a Plastometrex indentation plastometer, this uses a millimetre scale round indenting tip and measures the indent profile, with FE analysis to derive material properties. As the sampling area is much larger than the SIMM it should be able to provide more accurate results for materials that have higher levels of porosity. Fresh samples that are designed so that they can be measured in this way have been prepared and will be used to evaluate the plastometer for this application.

REFERENCES

[1] Beamler, “Scalmalloy: high performance aluminum for 3D printing,” Beamler, 20 August 2020. [Online]. Available: https://www.beamler.com/scalmalloy-high-performance-aluminum-for-3d-printing/. [Accessed 16 December 2022].

[2] J. Thurn, D. J. Morris and R. F. Cook, “Depth-sensing indentation at macroscopic dimensions,” *Journal of Materials Research,* vol. 17, no. 10, pp. 2679-2690, 2002.

[3] B. Roebuck, M. Stewart and M. Brooks, “DEPC-MN 30: Mapping Indentation Hardness,” NPL, Teddington, 2005.